Evidence for indurated sand dunes in the Martian north polar region

Volker Schatz,[1] Haim Tsoar,[2] Kenneth S. Edgett,[3] Eric J. R. Parteli,[1] and Hans J. Herrmann[1,4]

Received 18 June 2005; revised 29 October 2005; accepted 19 January 2006; published 28 April 2006.

[1] We investigate the relevance of induration as an explanation for the occurrence of dunes of unusual morphology in the Martian north polar region. The evidence for induration of aeolian deposits on Mars is reviewed. An explanation for rounded, elongated barchans in Chasma Boreale is presented. The role played by induration in the formation of linear dunes is discussed. Our arguments are supported by the results of a computer simulation model.

Citation: Schatz, V., H. Tsoar, K. S. Edgett, E. J. R. Parteli, and H. J. Herrmann (2006), Evidence for indurated sand dunes in the Martian north polar region, *J. Geophys. Res.*, *111*, E04006, doi:10.1029/2005JE002514.

1. Introduction

[2] The morphology and proximity of differing morphologies of a suite of eolian dunes in the Martian north polar region defy traditional explanation. The most basic control on eolian dune morphology is the nature of the wind regime. Unidirectional winds result in creation of barchan and transverse dunes, depending upon sediment supply; bidirectional wind settings result in linear, or seif, dunes; and multidirectional winds create star dunes [*Fryberger and Dean*, 1979]. The bidirectional and multidirectional winds that create linear and star forms, respectively, are typically the product of seasonal variation in wind direction [e.g., *Tsoar*, 1989; *Lancaster*, 1989]. Local topography can create localized wind conditions that result in trapping and building of large, complex dune forms, such as the Kelso dunes of southern California [*Sharp*, 1966].

[3] Unusual features occur in a dune field in Chasma Boreale, in the Martian north polar region. The white ellipse in Figure 1 shows the location of the dunes in this broad polar trough. Figure 2 shows examples of the dunes, as seen by the Mars Global Surveyor (MGS) Mars Orbiter Camera (MOC). In this dune field, linear and barchan dunes occur together, side-by-side and in some cases are merged to create a single bed form. The linear dunes lack the sinuosity commonly associated with terrestrial seif dunes [*Tsoar*, 1989]; in other words, these linear features are straighter than their counterparts on Earth. Furthermore, the dunes present an additional puzzle; the barchans are elongated into elliptical forms, and the slip faces are typically small or nonexistent (Figure 3).

[4] The elliptical and rounded barchans are reminiscent of forms, described by *Kerr and Nigra* [1952], that were created artificially by spraying advancing barchan dunes in Saudi Arabia with crude oil to halt their movement (Figure 3). As new sand arrived at the oil-soaked barchans from upwind sources, each dune became slightly more elongated, its slip face slightly smaller, as oil was sprayed on the dune in successive stages until all motion was stopped. The dunes in this case progressed, in stages, from a typical, crescent-shaped form to a rounded, elliptical dome-shaped form.

[5] The purpose of the study reported here was to investigate whether it is plausible that the rounded, elliptical dunes in Chasma Boreale could be the product of a process similar to that which was created by successive soaking of dunes in Saudi Arabia with crude oil, and whether the explanation might somehow extend to the occurrence of linear forms in the same dune field. Rather than anthropogenic processes halting dune movement in successive stages, as in the *Kerr and Nigra* [1952] example, we examine whether induration of dune sand may lead to production of dune forms in Chasma Boreale. Our exploration does not only apply to dunes in the north polar region of Mars; other examples occur in a variety of settings, including some at equatorial latitudes (Figure 4).

[6] While basic, typical dune morphologies are a product of wind regime (with, on Earth, contributions from vegetation and moisture) we conclude that induration may be an additional factor that influences morphology of dunes on Mars.

2. Methods

[7] Soaking a terrestrial dune with crude oil, to experimentally repeat the observations described by *Kerr and Nigra* [1952], was not a viable option as we undertook our study of the Chasma Boreale dunes. Instead, we chose a more environment-friendly approach. First, we examined

[1]Institute for Computational Physics, Stuttgart University, Stuttgart, Germany.
[2]Department of Geography and Environmental Development, Ben Gurion University of the Negev, Beer Sheva, Israel.
[3]Malin Space Science Systems, San Diego, California, USA.
[4]Departamento de Física, Universidade Federal do Ceará, Fortaleza, Brazil.

0148-0227/06/2005JE002514$09.00

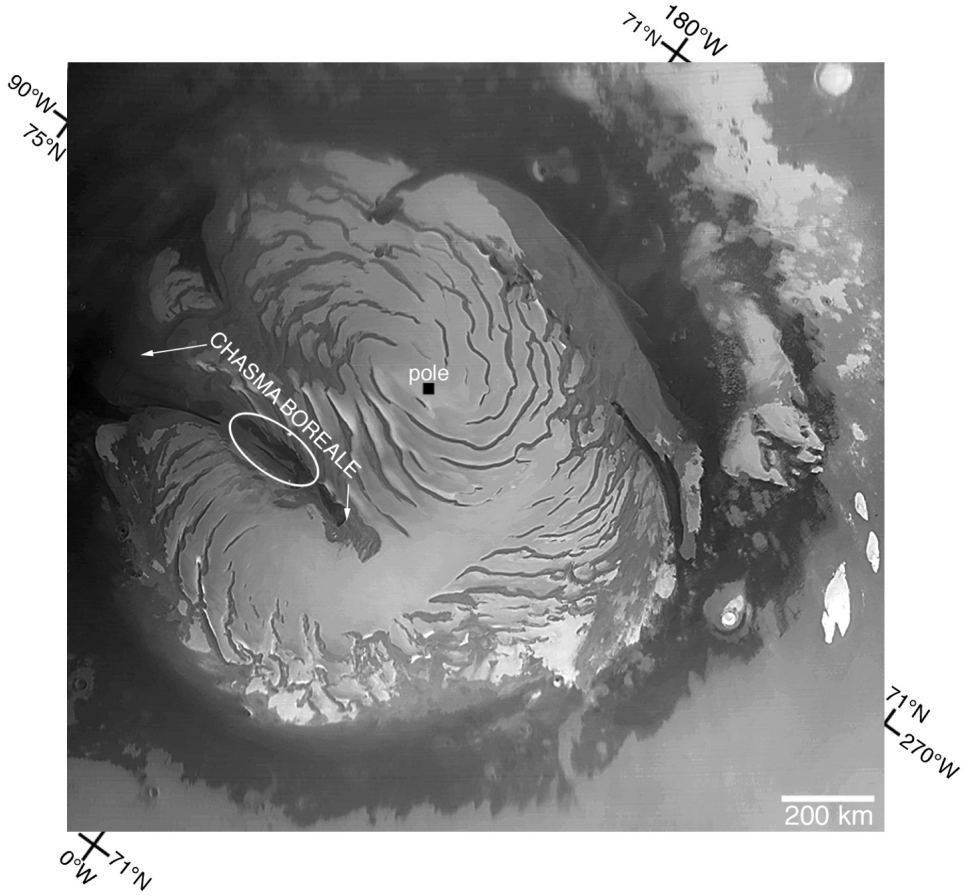

Figure 1. Polar stereographic view of the Martian north polar region as viewed in MGS MOC red wide-angle image FHA-00710. The locations of the dunes investigated in this work are enclosed by the white ellipse. The extent of Chasma Boreale is indicated by the arrows.

and reviewed all of the narrow angle images acquired by the MGS MOC from September 1997 through March 2005 for evidence regarding (1) whether Martian eolian dunes are moving distances great enough to be recorded by spacecraft cameras over the 1–1.5 Martian decades, and (2) whether any dunes exhibit evidence for indurated or crusted sediment. Second, having found evidence for induration and lack of movement among the Martian dunes, we used a well-developed and tested computer model [*Sauermann et al.*, 2001; *Kroy et al.*, 2002; *Schwämmle and Herrmann*, 2003, 2004, 2005], rather than crude oil, to simulate the progressive induration of a barchan dune under Martian conditions. Further, we applied the model to the linear dune case, in an effort to understand how these can coexist with the barchan forms in the Chasma Boreale region.

3. Setting of the Chasma Boreale Dunes

[8] The dunes in Figures 2 and 3 are in Chasma Boreale, primarily between latitudes 83° to 85°N, longitudes 14° to 42°W (Figure 1). The entire north polar cap is nearly surrounded by aeolian dune fields [*Tsoar et al.*, 1979]. The dunes spend more than half a Mars year covered by seasonal carbon dioxide frost. The frost forms in early autumn and persists through winter and much of spring. By late spring and early summer, however, the frost is gone and the dunes are exposed to the atmosphere and are occasionally subjected to winds of sufficient magnitude to raise dust and manifest themselves as dust storms [e.g., *Cantor et al.*, 2001]. Like all other Martian dunes, the sands have a low albedo. Knowledge of their composition is incomplete, but they are generally thought to have a mafic to intermediate silicic composition [*Bandfield*, 2002]. Recent near-infrared observations by the Mars Express OMEGA instrument suggests that gypsum is present among the silicate grains in at least a portion of the north polar sand sea [*Langevin et al.*, 2005]. The sand in Chasma Boreale does not exhibit the gypsum signature, at least in the initial OMEGA results. Chasma Boreale sands appear to be derived from the erosion of a suite of sand-rich layers exposed in the bounding scarps near the head of the chasm [*Edgett et al.*, 2003; *Fishbaugh and Head*, 2005].

4. Martian Dune Movement and Induration

[9] Crusting or induration of regolith fines and eolian bed forms has been observed at all five successful Martian landing sites, Viking 1, Viking 2, Mars Pathfinder, Spirit, and Opportunity [e.g., *Arvidson et al.*, 1989, 2004; *Moore et al.*, 1999; *Thomas et al.*, 2005]. Figure 5 shows an example

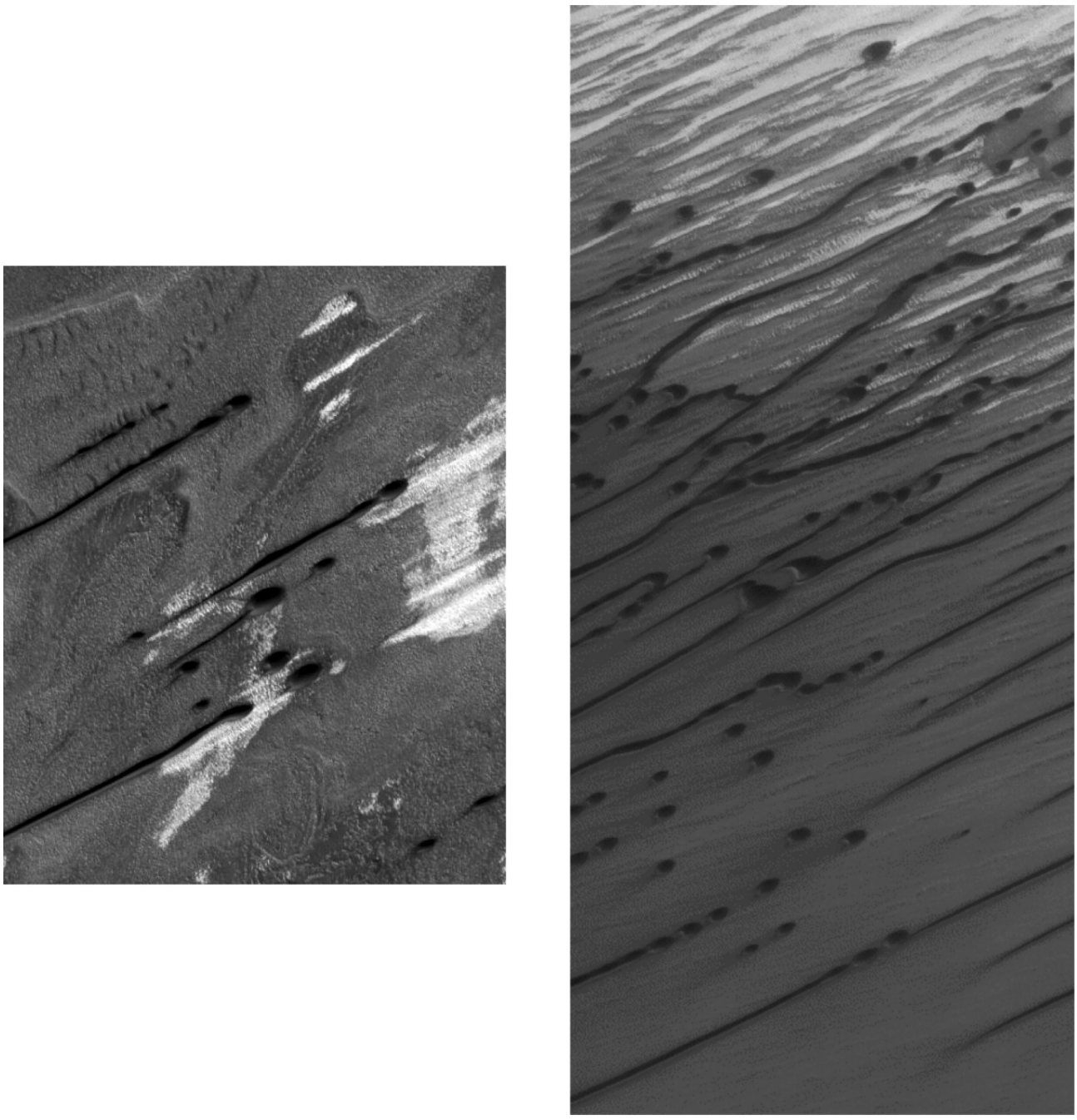

Figure 2. Subframes of MGS MOC images showing examples of the elongated, rounded barchans and linear dunes in Chasma Boreale. Both images cover areas about 3 km wide. (left) From image E01-00104, located near 83.9°N 40.5°W. (right) From MOC image S02-00901, located near 84.2°N 37.9°W. In both cases, sand transport has been from the upper right toward the lower left.

in which the wheels of the rover, Opportunity, broke through and slightly rotated blocks of a crust formed of cemented grains at and near the surface of a large eolian bed form on Meridiani Planum. Work done following the Viking lander missions of the 1970s proposed that crusts may form as water vapor diffuses into and out of the fine-grained materials on the planet's surface; salts would be deposited as an intergranular cement [*Clark et al.*, 1982; *Jakosky and Christensen*, 1986].

[10] The landers and rovers did not visit any of the classic, low albedo Martian dunes. To find evidence regarding whether any Martian dunes are indurated, we examined the highest spatial resolution images available; that is, images of 0.5 to 15 m per pixel resolution acquired by the MGS MOC. We searched every MOC narrow angle image acquired between MGS orbit insertion in September 1997 and the end of March 2005, the latest period for which data have been archived with the NASA Planetary Data System as of this writing. We were particularly interested in

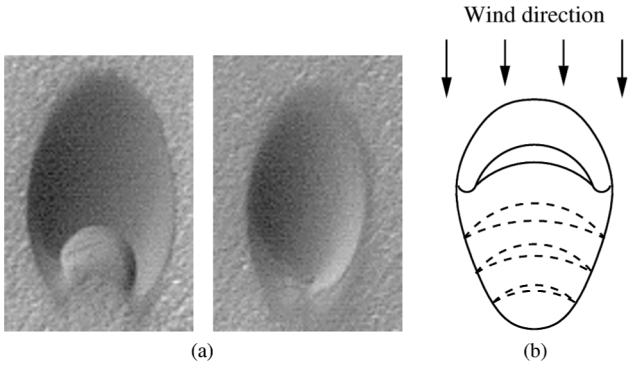

Figure 3. (a) MGS MOC images of a rounded barchan and a dome dune located near 84.9°N 26.6°W, in image M02-00783. The shown parts of the image are each approximately 240 m wide. (b) Sketch of the deposition in the lee of an oil-soaked barchan [after *Kerr and Nigra*, 1952]. The initial barchan and the final shape are drawn; the dashed lines show the positions of the slip face in intermediate stages, until an elliptical, dome-like shape is produced.

the images of eolian dunes, including those in which dunes were imaged more than once by MOC and imaged earlier by the cameras on board the orbiters Mariner 9, Viking 1, and Viking 2.

[11] While Martian dunes generally appear to be fresh and have no superimposed impact craters [*Marchenko and Pronin*, 1995], the presence of which would imply antiquity, repeated imaging by MOC has shown no clear evidence for translation of eolian dunes across the Martian surface. Terrestrial experience dictates that the smallest dunes are the ones expected to move the farthest in the shortest amount of time [e.g., *Finkel*, 1959; *Long and Sharp*, 1964; *Hastenrath*, 1967]. MOC images were acquired of all of the smallest dunes resolved in images by the Mariner 9 and Viking orbiters (e.g., Figure 6), and no evidence for movement was observed (however, the spatial resolution of the Viking and Mariner images were typically in the 8–50 m/pixel range, thus limiting the ability to detect dune movement to ≈1 pixel in the earlier images). No evidence for translation of small (or large) dunes across a surface over time intervals spanning 4–15 Martian years has been observed. An example comparing the highest resolution view of dunes obtained by the Viking 1 orbiter with new views of the same dune field as seen by MGS is shown in Figure 6. These results are consistent with earlier reports by *Edgett and Malin* [2000], *Edgett* [2002], and the eolian megaripple study by *Zimbelman* [2000]. As illustrated by the example in Figure 7, seasonal deposition of dust on low albedo dunes, and removal of the dust by dust devils rather than saltation of the sand under influence of wind gusts and storms, is another indicator that Martian dunes are generally inactive, relative to terrestrial desert examples.

[12] While it appears that dunes have generally not been moving in the past few Martian decades (or are moving at a rate too low to be measured, given the constraints on image spatial resolution and sporadic coverage by orbiting spacecraft, during this interval), this is not evidence for induration of the bed forms. Several dunes exhibit features that indicate ways in which Martian dunes may be immobilized. On Earth, increased moisture, decreased wind power, and the growth of vegetation are contributors to immobilization. Another way to immobilize a dune is to bury it rapidly enough that it can no longer move. While the rate of dune burial is unknown, Figure 8 shows one clear example and several other probable examples of dunes that have been buried and embedded within ice of an outlier of the residual north polar cap. In other words, the dunes in Figure 8 are encased within ice that is permanent in the sense that it has not been removed from the area during the entire period that orbiting spacecraft have been examining the planet (1972–2005); the dunes remain encased in ice during the summer season.

[13] Finally, MOC images also show landforms strongly suggestive of crusting or induration of the sediment. The best examples are dunes with grooved surfaces [*Edgett and Malin*, 2000]. Figure 9 shows two examples, one from Herschel Basin, the other from a dune field in Nili Patera. Winds have scoured the indurated dune surfaces to form, essentially, small yardangs. Figure 10 shows another form of evidence for indurated sand dunes: steep-walled avalanche chutes and gullies formed on dune slip faces. In dry, unsolidated dunes, slip faces occur at the angle of repose; the walls of the chutes and gullies cut into the slip faces in Figure 10 are steeper than the angle of repose.

5. Simulations

[14] Images from landers and rovers show that crusting of surface fines is a common phenomenon on Mars (e.g., Figure 5). Orbiter images suggest that Martian dunes have

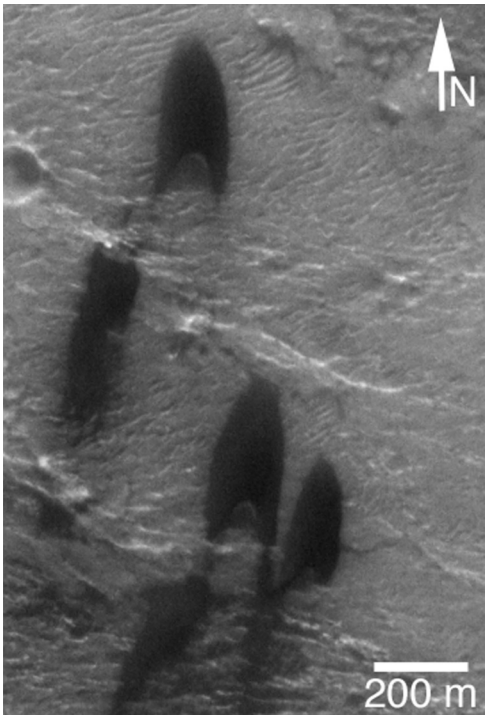

Figure 4. Elongated barchan dunes in an equatorial setting. This is a subframe of MOC image R14-01173, located near 8.8°S, 271.1°W.

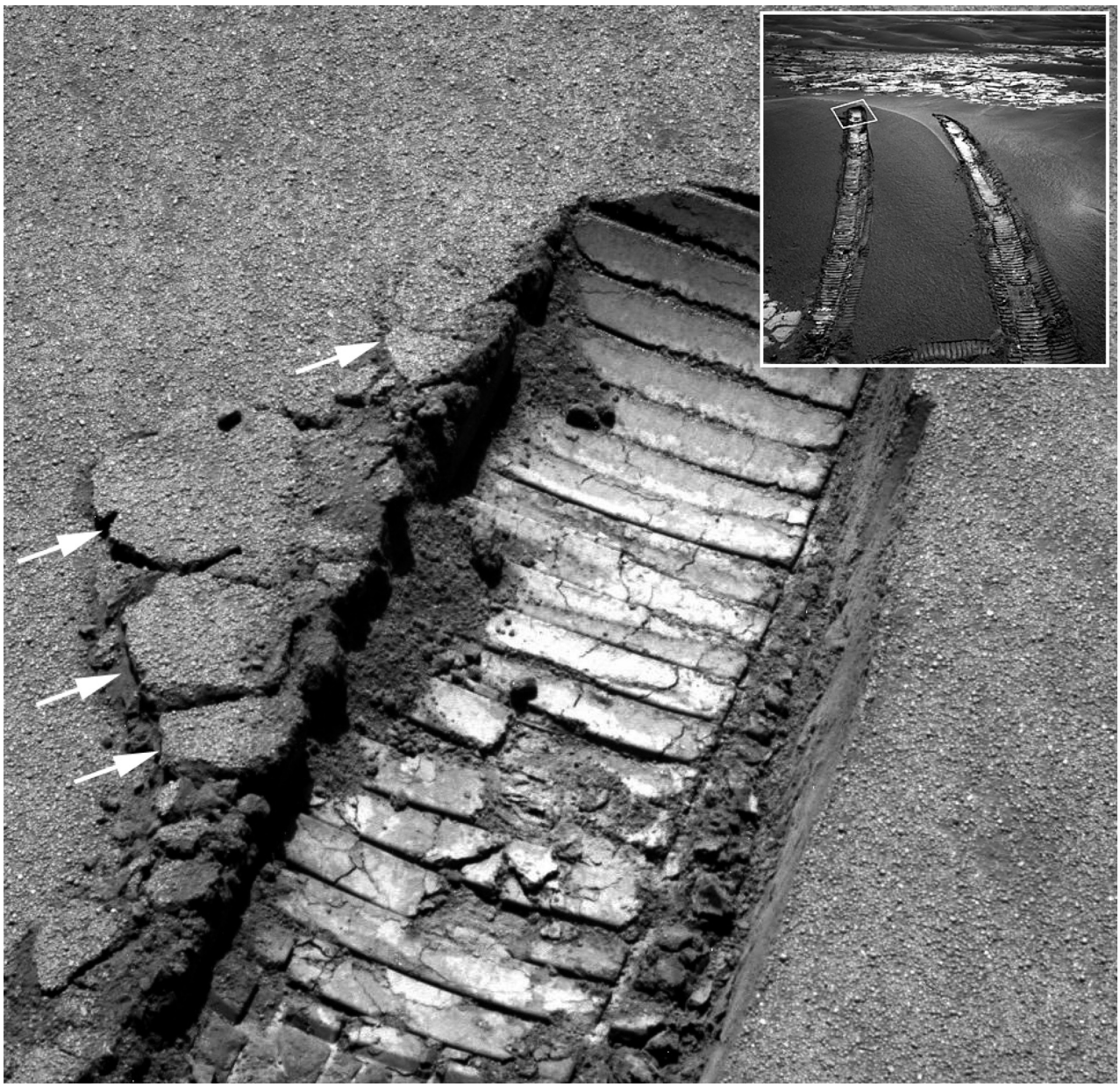

Figure 5. A ≈16 cm wide wheel track cut into the surface of an eolian megaripple at the Mars Exploration Rover, Opportunity site on Meridiani Planum. The arrows point to blocks of broken, crusted sand disrupted by the action of the rover wheels. The white box in the inset shows the context of this image, near the crest of the large ripple. The picture is a subframe of a 432 nm left Pancam image, 1P181893282EFF62FYP2392L7M1. The image was acquired on Sol 605 (6 October 2005) at approximately 1149:03 Mars local solar time. The picture is from a prearchival public release product credited to NASA/Jet Propulsion Laboratory/Cornell University. The inset is a right Navigation Camera image, 1N181898466EFF62GMP1832R0M1, acquired on Sol 605 near 1313:07 Mars local solar time, from a prearchival public release product credited to NASA/Jet Propulsion Laboratory.

generally not been moving in recent decades (Figure 6), and some exhibit features, visible from orbit, that are attributable to crusting or induration (Figures 9 and 10). The dunes in the Chasma Boreale region were not imaged by Mariner 9 or Viking at a spatial resolution adequate to see them and measure their movement by comparison with MOC images. Some of the dunes have, however, been repeatedly imaged by MOC during the past four Martian years, and, again, show no evidence for movement (Figure 11). The Chasma Boreale dunes also do not exhibit grooves or steep-walled avalanche chutes. However, the rounded barchans do resemble the oil-soaked dunes of *Kerr and Nigra* [1952], and the linear dunes simply should not occur with the barchans, unless they are unlike terrestrial linear dunes, and formed, somehow, in a unidirectional wind regime. In this section, we explore the question of sand induration through com-

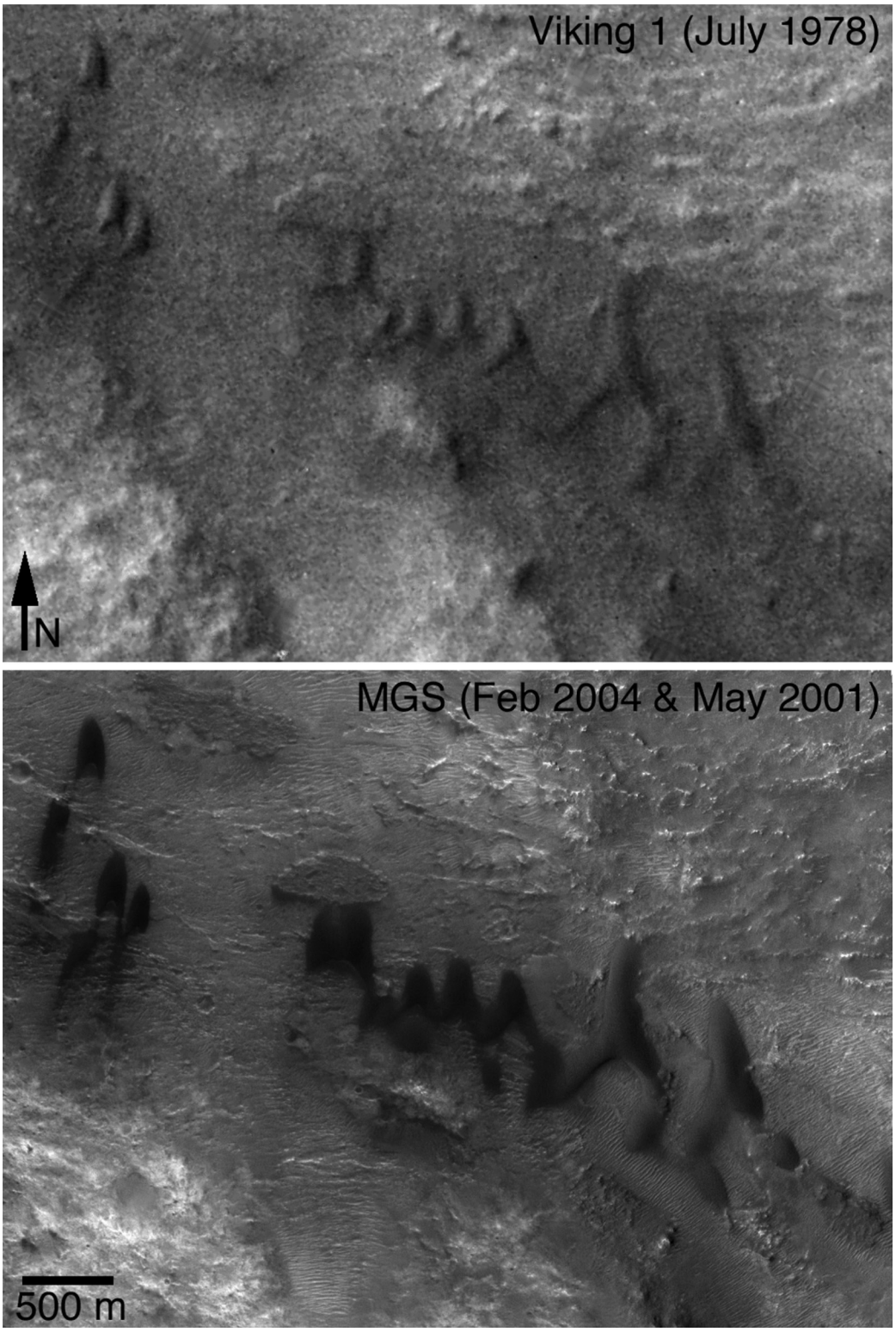

Figure 6. Martian eolian dunes have not been observed to have moved in recent decades. This is an example that compares an image of small dunes observed by the Viking 1 on 12 July 1978 with the same dunes as observed by Mars Global Surveyor on 10 February 2004 (left two thirds of bottom image) and 27 May 2001 (right third of bottom image). The interval between July 1978 and May 2001 is ≈12.2 Mars years; between July 1978 and February 2004, it ≈13.7 Martian years. The Viking picture is a subframe of 755a19; the MGS Mars Orbiter Camera images are subframes of E04-02207 and R14-01173. These dunes are located near 8.8°S, 271.1°W.

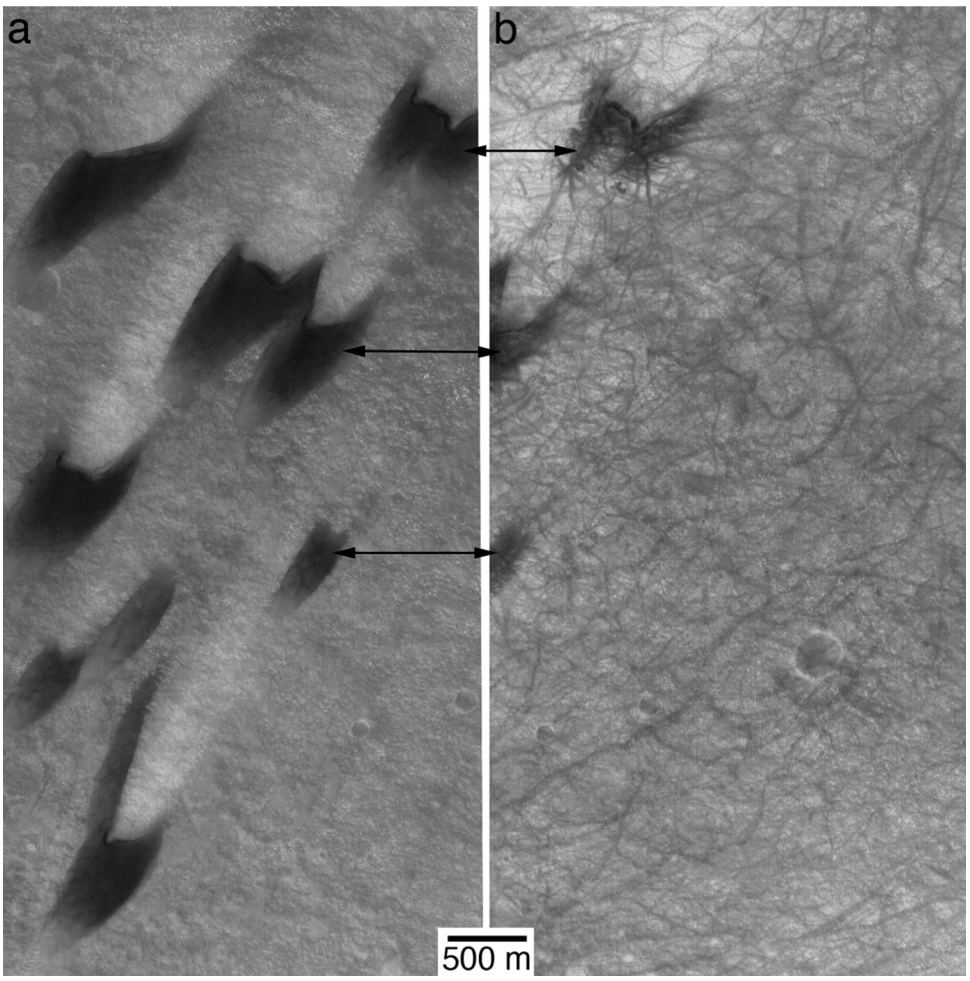

Figure 7. Illustration of general inactivity of modern dunes, in part, by examples of dunes that are seasonally coated by dust, settled from the atmosphere. Active dunes, upon which saltation is occurring, would clean themselves of any dust that settles upon them. In this example, from Arkhangelsky Crater near 41.2°S, 24.8°W, dust is known to cover the dunes because dust devils have created streaks by removing or disrupting some of the coating on the dunes. (a) View of the dunes during early summer (L_s 290.5°) in a subframe of MOC image R10-05441. If active, the dunes would be completely dark and not exhibit dust devil streaks. (b) How the dunes typically look in late spring (L_s 268.8°), with a thicker, more extensive dust coating and dust devil streaks. This is a subframe of E10-01286, taken ≈1.1 Mars years earlier but only ≈0.1 Mars year earlier in terms of season, relative to the first picture. Dust devils appear to be the main contributor to the darkening of the dunes as the season passes from spring to summer.

puter simulation of the creation of the observed bed form morphologies.

[15] Sand dunes have for decades attracted the attention not only of geomorphologists and geologists, but also of physicists and mathematicians [e.g., *Bagnold*, 1941; *Fowler*, 2001]. Sand transport processes have been investigated at small scales in order to gain knowledge about the formation, wandering and evolution of dunes. In particular, our understanding of saltation has been steadily refined [*Owen*, 1964; *Anderson and Haff*, 1991; *Nalpanis et al.*, 1993; *Sauermann et al.*, 2001; *Andreotti*, 2004].

[16] Computer simulations on the basis of these insights have shed light on processes observed in the field at the scale of dunes and dune fields [*Anderson and Haff*, 1988; *Schwämmle and Herrmann*, 2003; *Hersen et al.*, 2004]. The advantage of this approach is that it can be transferred with ease to a different environment, such as on Mars. It is believed that saltation is the dominant transport process responsible for dune formation also on Mars, and Martian dunes have been successfully simulated using saltation models [*Parteli et al.*, 2005].

[17] The simulations presented here are key to our case that the rounded, elongated, slipfaceless dunes in Chasma Boreale owe their morphology to the contribution not only of a unidirectional wind regime, but also the successive induration of sand at each stage of slip face advancement. Geological arguments derive from our experience and observation of geological processes on Earth. This knowledge, though extensive, may not in its entirety be applicable in a completely different environment such as Mars. While the mechanisms of sand transport on Mars are acknowledged to be the same as on Earth, the detailed

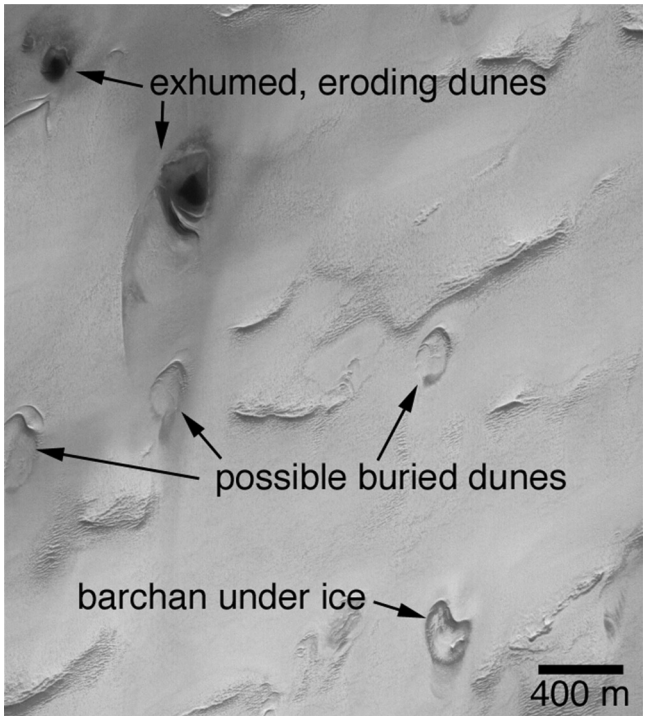

Figure 8. Dunes trapped and frozen beneath ice in an outlier of the Martian north polar cap. One semiexhumed barchan is clearly recognizable near the bottom of the image. A small remnant of the material that must have once completely buried the dune is seen on the southeast (lower right) slope of the frozen barchan. Other possible buried, frozen dunes are indicated. In the northwest corner of the image (top left), two dark patches indicate the location of dune sand that has been subjected to erosion, after buried dunes were exhumed and sand motion was reactivated. This is a subframe of MOC image R23-00350, located near 79.2°N, 226.9°W.

shape of the resulting dunes differs. Because we here are investigating landforms which do not occur naturally on Earth, we have to look specifically into the factors that can cause these differences and the factors that remain the same. This question can be answered by physics: The laws of physics are universal and therefore apply under any conditions, including Mars. What distinguishes the situation on Mars, however, is the value of physical constants, like gravity (g = 3.71 m/s), the density of the atmosphere (ρ_{fluid} = 0.02 kg/m^3) and of the sand grains (ρ_{grain} = 3200 kg/m^3), the wind shear velocity (u_* = 4 m/s) and its threshold for aeolian entrainment (u_{*ft} = 2.65 m/s) and sustained saltation (u_{*t} = 2.0 m/s) [*Iversen and White*, 1982; *Sullivan et al.*, 2000].

[18] A few years ago, a physical model of saltation sand transport was developed by *Sauermann et al.* [2001], *Kroy et al.* [2002], and *Sauermann* [2001]. This model has been implemented as numerical simulation software. It allows us to transfer our knowledge of dune formation to different environments in a physically meaningful way; the physics laws implemented in the program remain the same while the values of physical quantities can be adapted. We used the simulation software to test our hypothesis, and the results described below support our arguments. Beyond the physical constants already presented above, we used the following parameters: The grain diameter d_{grain} = 500 μm [*Edgett and Christensen*, 1991, 1994], the drag coefficient of the grains C_d = 1.5 [*Owen*, 1964], the angle of repose 33° [*Greeley et al.*, 1999] and the roughness length of the inflow profile with respectively without saltation (1 mm respectively 50 μm). The parameters of the saltation model were chosen as in a previous simulation of Martian dunes by *Parteli et al.* [2005], with the exception of α = 0.53. We would like to state that our value for the wind shear velocity of 4 m/s is consistent with estimated friction speeds at the Viking 1 lander site for a case in which fines were observed to have been moved [*Moore*, 1985], and with observations of dust storms and clouds in the north polar region [*Cantor et al.*, 2001, 2002]. The mathematical models involved in the dune simulation software are briefly summarized in Appendix A.

5.1. Rounded Barchans

[19] Elongated, elliptical, dome-shaped dunes, such as those in Figures 2, 4, and 11, might be the product of successive induration as the slip face advances forward and becomes smaller and smaller, until it disappears, as was observed by *Kerr and Nigra* [1952] for oil-soaked barchans on Earth. In the Saudi Arabia case, the dunes were sprayed with oil, then additional sand arrived at the fixed dune, blew over its top, and became deposited on the lee side, whereupon the dune was again sprayed with oil. This process continued and, over time, the slip face of each dune became successively smaller, and the dune more rounded and elliptical. This is not typical behavior for lee-side deposition of sand in a dune field, but is a product of the process of successively inhibiting sand movement, in this case, using oil, on the main body of each dune.

[20] The similarity of the oil-soaked dunes to the rounded forms on Mars suggests that the Martian examples could have formed in a similar way, with ice, frozen carbon dioxide, or mineral salts taking the place of oil as the cause for induration. To test the hypothesis under conditions suitable for Mars, we simulated the process of forming a successively indurated barchan using the appropriate parameters for Mars. Figure 12 shows the successive stages of deposition in the lee of the fixed barchan. The shape of the initial dune and the latter successions were all simulated with the same atmospheric conditions, particle properties, and wind speed; the only change was to simulate induration

Figure 9. Eolian dunes considered to be crusted or indurated because wind erosion has scoured grooves into their surfaces. (a) Example from Herschel Crater, located near 15.3°S, 228.3°W. This is a subframe of MOC image M00-03222. (b) Example, less thoroughly grooved than the dunes in Herschel, from a dune field in Nili Patera caldera in Syrtis Major. This subframe of MOC image S04-00433 is located near 8.8°N, 292.8°W.

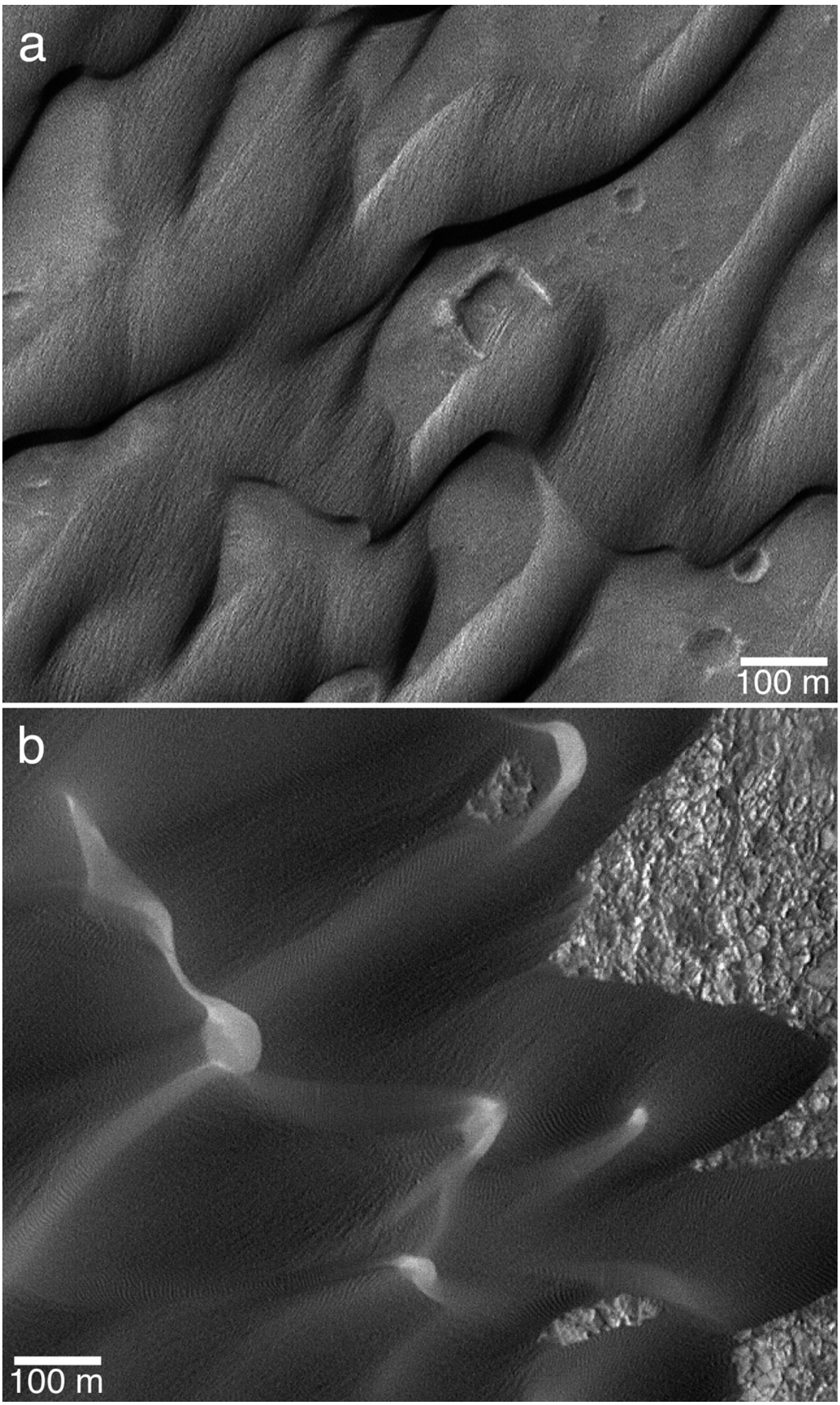

Figure 9

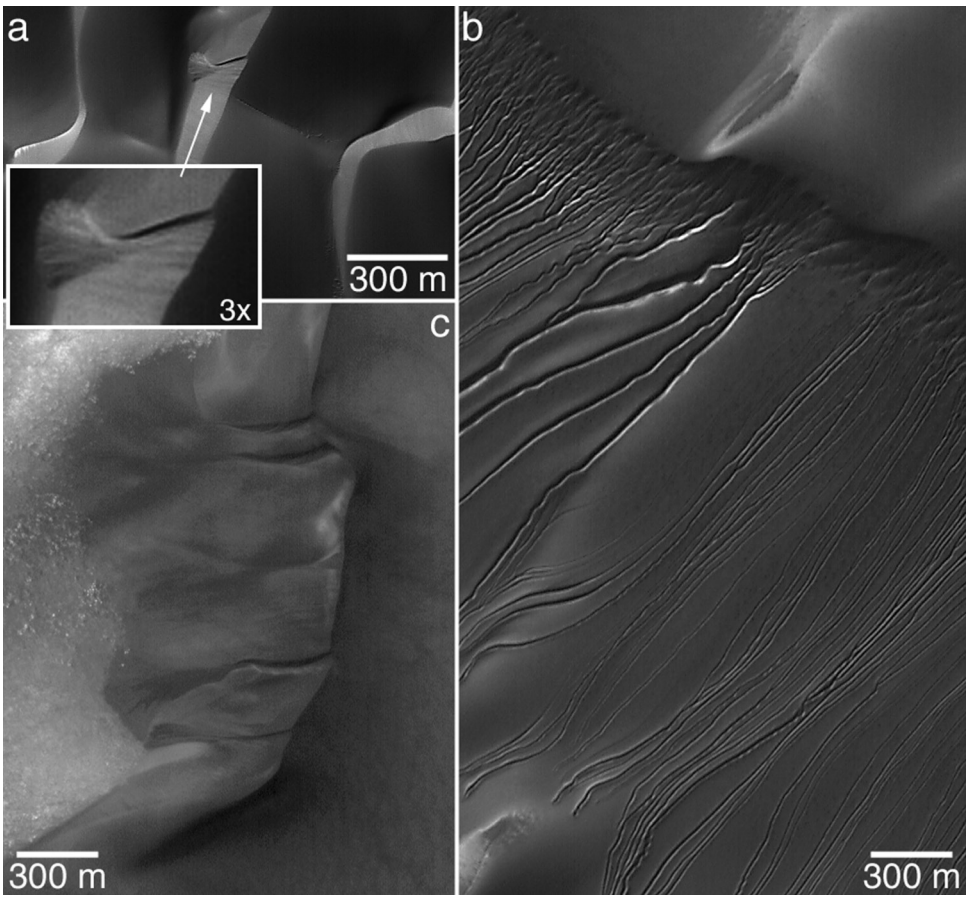

Figure 10. Evidence for induration or crusting of Martian eolian dune sands, in the form of steep-walled slip face avalanche scars and chutes. (a) Example from dunes in Rabe Crater, near 44.1°S, 325.6°W, in subframe of MOC image M21-01006. (b) Example showing gullies on dune slip face and sharp erosional forms near slip face/brink interface, on large dune in Russell Crater, near 54.5°S, 347.3°W, in subframe of MOC image E02-00894. (c) Avalanche chutes on dune slip face in Kaiser Crater. This is a subframe of MOC image M13-01025, located near 47.3°S, 340.4°W.

(non mobility) of each successive stage of the dune development, while at the same time adding new sand from the upwind direction.

[21] Some small differences between the simulation in Figure 12 and the satellite image (Figure 3a) have to be discussed. In the simulations, the brink of the initial barchan is still visible at later stages. In reality, this visible ridge would be slowly eroded even if the dune was indurated. The second discrepancy is that the slip face in the photo appears to be very long, but the foot of the slip face is hard to discern, and a slip face extending nearly to the end of the horns would imply a very high slip face brink, which would be in contrast with the flat rounded shape suggested by the shadows and with the height of other Martian dunes described by *Bourke et al.* [2004]. The aspect ratio (height divided by length) of our simulated dunes is consistent with the results of *Bourke et al.* [2004].

5.2. Chasma Boreale Linear Dunes

[22] In addition to the dome-shaped barchans, the region near the Martian north pole exhibits linear dunes that are very straight, unlike their meandering counterparts on Earth [*Tsoar*, 1982, 1983, 1989]. These linear dunes occur with the domes and rounded barchans, suggesting that they form in winds flowing parallel to the linear dunes, yet terrestrial experience requires two oblique winds, not a single, unidirectional wind, to create such bed forms.

[23] MGS MOC narrow angle images show that the upwind end of the linear dunes, immediately downwind of the domes, shows a knotted structure (e.g., Figure 13). We have performed a computer simulation of such dunes, starting from a straight ridge in wind direction located just downwind of an unerodable dome. As can be seen in Figure 14, the knots at the upwind end are reproduced in early steps of the simulation. Their formation is analogous to the instability of a sand bed under unidirectional winds [e.g., *Andreotti and Claudin*, 2002; *Schwämmle and Herrmann*, 2004]. Later on, however, the simulated linear dune decays into a string of barchans. That this has not happened in Chasma Boreale can be explained if the linear dunes are indurated or were formed by erosion in the first place. Although our simulations do not show how the linear forms were initiated, they do suggest (as in the case of the elongated, dome-shaped barchans) that the sands are presently or very recently indurated.

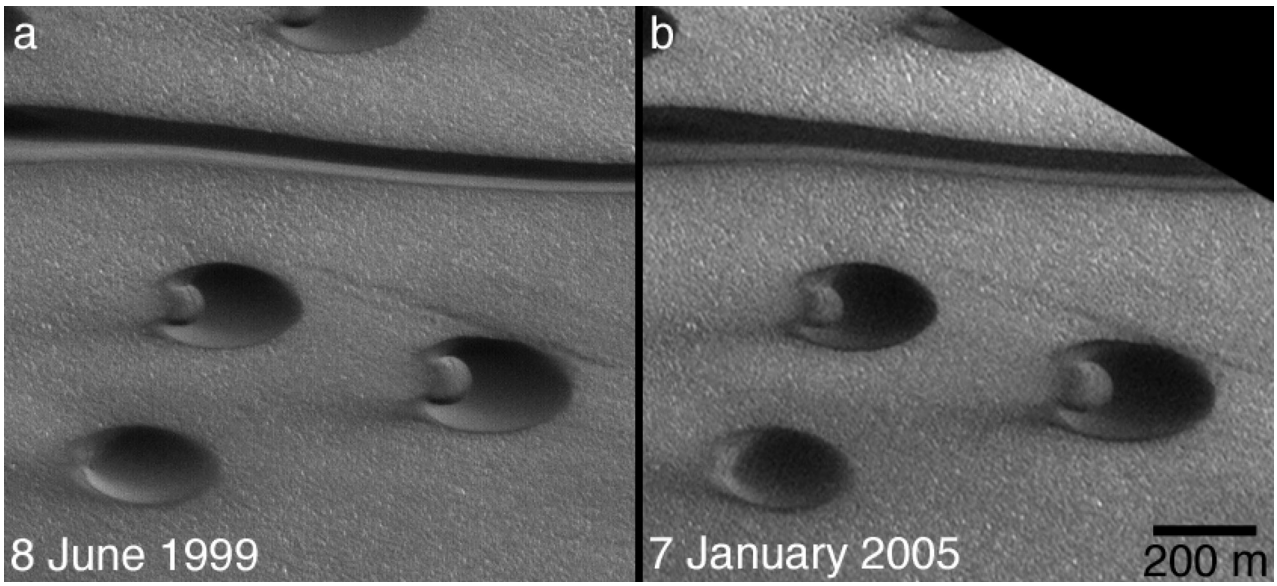

Figure 11. Rounded barchans of Chasma Boreale imaged repeatedly by the MGS MOC during the past several Martian years. Relative to features on the substrate across which they are moving, the dunes do not appear to have moved during the mission. The interval between acquisition of the two images shown here is 2.97 Mars years. These dunes include the two shown in Figure 3. (a) Subframe of MOC image M02-00783. (b) Subframe of MOC image S02-00302. The dunes are illuminated by sunlight from the lower left and are located near 84.9°N, 26.6°W.

5.3. Parameter Dependence and Significance of the Simulation Results

[24] How much our results depend on the specific values of the parameters chosen is a question which is difficult to answer quantitatively. Because of the large number of parameters, a systematic investigation would at present be prohibitively expensive in terms of computational time. However, what can be said both from experience and from the continuity of the mathematical functions involved is that small changes in some parameter values do not change our results significantly. The speed with which the lee side of the barchans fills up or with which the linear dunes are reshaped changes slightly, but the resulting bed forms remain the same.

[25] Completely different sets of parameters exist which lead to qualitatively similar results; for instance, it is possible to simulate the experiment of *Kerr and Nigra* [1952] on Earth. However, for that purpose all parameters have to be adapted to the different ambient conditions. It is not possible to change only one simulation parameter significantly and still to obtain the same results. Therefore our simulation results are not a triviality but reflect physical reality under the conditions defined by the chosen set of parameters.

6. Conclusions

[26] Observations from landed spacecraft show that crusting of Martian regolith fines and eolian bed forms has occurred. Images acquired from orbit, particularly those of aerial photograph scale obtained by the Mars Global Surveyor MOC, provide geomorphic evidence that many, if not

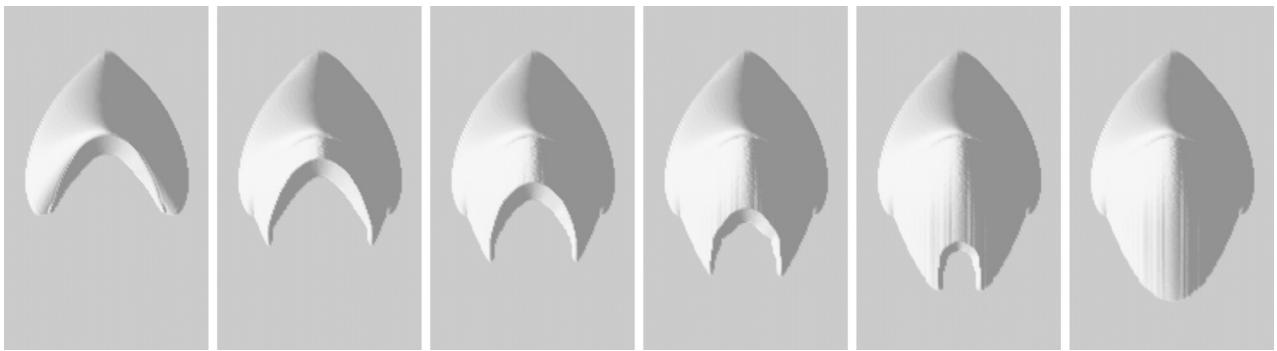

Figure 12. Successive stages of evolution of deposition in the lee of an indurated barchan on Mars. The length of the shown region is 400 m, the width 240 m. The first picture shows the initial barchan.

all, Martian eolian dunes are presently crusted or indurated. Unlike their terrestrial counterparts, which can move many tens of meters in a decade or less, small Martian dunes do not appear to have moved on timescales of the order of 3–15 Martian years. Grooved surfaces on some dunes, and steep-walled avalanche chutes on others, are key indicators that Martian dunes are indurated.

[27] The Martian north polar region, particularly within Chasma Boreale, presents another form of evidence for dune induration. While wind regime is the primary determinant of dune morphology on both Earth and Mars, induration may be a secondary contributor that, in the case of Chasma Boreale, has led to creation of elongated, elliptical, dome-shaped dunes; elongated barchans with proportionally tiny slip faces; and straight (as opposed to sinuous, like seif dunes) linear dunes that coexist with barchan forms in a unidirectional, rather than bidirectional, wind regime. The hypothesis regarding induration of dunes in Chasma Boreale is supported by observations of artificially indurated dunes by *Kerr and Nigra* [1952] and computer simulation of eolian bed form development.

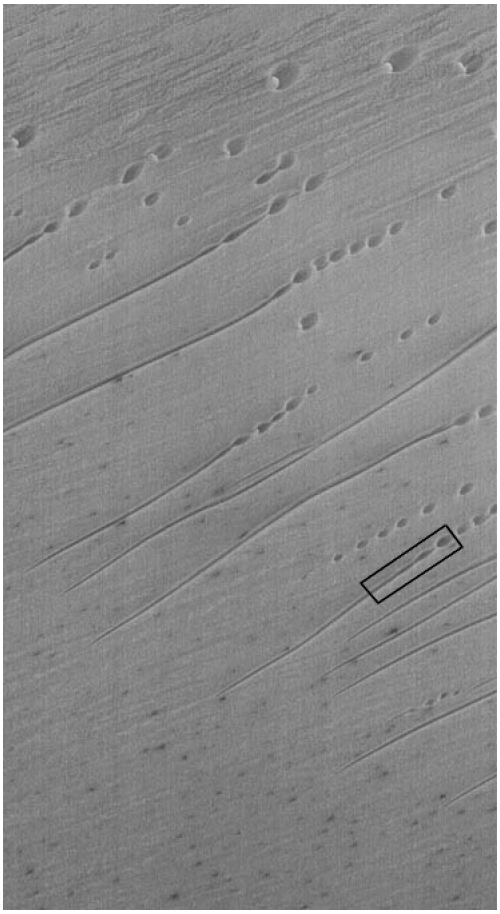

Figure 13. A field of linear dunes in Chasma Boreale. This is a part of MOC image E15-00784, located at 84.24°N, 39.95°W. It covers an area about 3 km across. The bright outlines of the dunes and of the ridges in the surrounding region indicate that they are covered by seasonal frost, most likely frozen carbon dioxide. The black rectangle indicates the region selected for our linear dune simulation (see Figure 14).

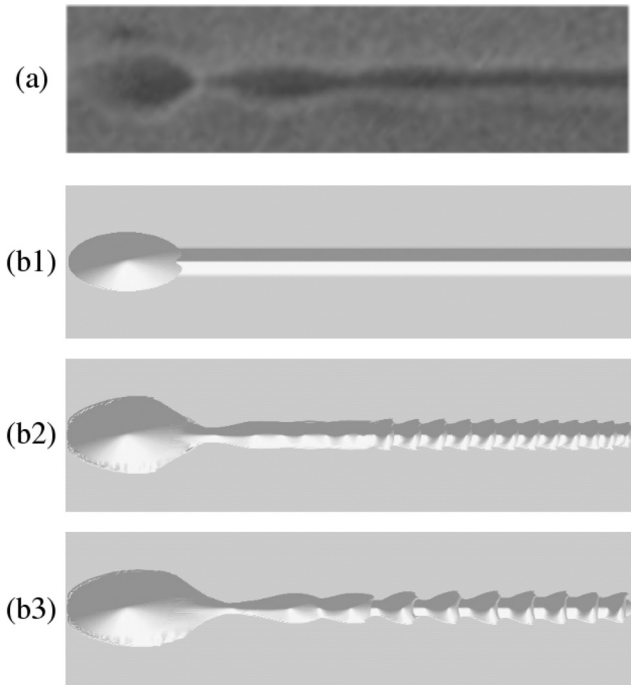

Figure 14. (a) A detail of Figure 13. (b) Simulation of the evolution of a straight linear dune downwind of a dome. Besides small variations in thickness, small barchans can be seen to develop, which are not observed on Mars. From this we conclude that the linear dunes in Figure 13 are indurated.

Appendix A

[28] This appendix will outline very briefly the mathematical models implemented in our simulation software. Not all the symbols will be explained; this appendix merely serves to present the model equations. For obtaining the information we omit here, we refer the reader to *Sauermann* [2001] and *Schwämmle and Herrmann* [2005]. They employ the same nomenclature as we do here and explain of all the quantities and derivations of the formulas.

[29] The height profile of the dunes and other physical quantities are represented in a discretized manner, that is, their values at points on a quadratic grid are stored in the computer. To simulate the evolution of sand deposits, the software computes several quantities in turn: The shear stress exerted on the ground by the wind, the mean velocity and density of the saltating grains, the sand flux and the resulting change in the height profile.

[30] The shear stress is computed according to an analytical work describing the perturbation of the ground shear stress by a low hill or dune [*Weng et al.*, 1991; *Hunt et al.*, 1988]. This perturbation is given by:

$$\begin{aligned} \tilde{\hat{\tau}}_x &= \frac{\tilde{h}_{\mathrm{sep}} k_x^2}{|\mathbf{k}|} \frac{2}{U^2(l)} \left\{ -1 + \left(2 \ln \frac{l}{z_0} + \frac{|k|^2}{k_x^2} \right) \sigma \frac{K_1(2\sigma)}{K_0(2\sigma)} \right\}, \\ \tilde{\hat{\tau}}_y &= \frac{\tilde{h}_{\mathrm{sep}} k_x k_y}{|\mathbf{k}|} \frac{2}{U^2(l)} 2\sqrt{2}\sigma K_1\left(2\sqrt{2}\sigma\right) \end{aligned} \tag{A1}$$

where

$$\sigma = \sqrt{i\, L\, k_x z_0 / l}.$$

This calculation is formulated in Fourier space and necessitates transforming the height profile and reverse-transforming the resulting shear stress. To compensate for an overprediction of the shear stress by these formulas (CERC1, Comparison ADMS 3.1 to Blashaval Hill Field data, available at http://www.cerc.co.uk/software/publications.htm and CERC2, Comparison ADMS 3.1 to Askervein Hill Field data, available at http://www.cerc.co.uk/software/publications.htm), we increase the imaginary part of τ_x compared to equation (A1).

[31] Flow separation at the slip face brink is taken into account by assuming an idealized "separation bubble", a region inside which there is no flow and outside of which the air flows as over a shape of the combined dune and bubble. The height profile h_{sep} in equation (A1) is the profile of the dune including the separation bubble.

[32] From the shear stress, the sand flux is computed according to *Sauermann et al.* [2001] and *Kroy et al.* [2002] with some modifications by *Schwämmle and Herrmann* [2005]. First the modification of the air flow due to the presence of saltating grains is accounted for. This results in an effective wind velocity driving the grains which was derived from the results of microscopic simulations of saltation [*Anderson and Haff*, 1991]:

$$\mathbf{v}_{\mathrm{eff}} = \frac{2}{\kappa}\frac{\boldsymbol{\tau}}{|\boldsymbol{\tau}|}\frac{1}{\sqrt{\rho_{\mathrm{fluid}}}}\left(\sqrt{\frac{z_1}{z_m}|\boldsymbol{\tau}| + \left(1-\frac{z_1}{z_m}\right)\tau_t}\right. \\ \left. + \frac{1}{2}\left(\ln\frac{z_1}{z_{0\ \mathrm{ground}}} - 2\right)\sqrt{\tau_t}\right). \quad \text{(A2)}$$

The shear stress $\boldsymbol{\tau}$ results from equation (A1) through $\boldsymbol{\tau} = \boldsymbol{\tau}_0 + |\boldsymbol{\tau}_0|\,\hat{\boldsymbol{\tau}}$, where $\boldsymbol{\tau}_0$ is the shear stress over a flat plane.

[33] The next step is the computation of the typical velocity of the saltating grains. It is determined by the balance between the drag force acting on the grains, the loss of momentum when they splash on the ground, and the downhill force. The balance of forces gives the following vector equation which is solved numerically:

$$\frac{3}{4}C_d\frac{\rho_{\mathrm{fluid}}}{\rho_{\mathrm{grain}}}\frac{1}{d_{\mathrm{grain}}}(\mathbf{v}_{\mathrm{eff}}-\mathbf{u})|\mathbf{v}_{\mathrm{eff}}-\mathbf{u}| - \frac{g}{2\alpha}\frac{\mathbf{u}}{|\mathbf{u}|} - g\nabla h = 0 \quad \text{(A3)}$$

[34] It remains to compute the saltating sand density ρ to obtain the sand flux $\mathbf{q} = \rho\mathbf{u}$. It is obtained by numerically solving the transport equation:

$$\mathrm{div}(\rho\mathbf{u}) = R_{\mathrm{salt}} + R_{\mathrm{aero}}, \quad \text{(A4)}$$

where

$$R_{\mathrm{salt}} = \frac{1}{T_s}\rho\left(1-\frac{\rho}{\rho_s}\right) \quad \text{for } \rho > \rho_s \text{ or } h > 0, \quad 0 \text{ otherwise;}$$

$$R_{\mathrm{aero}} = \beta\left(\frac{\tau - \rho\frac{g}{2\alpha}}{\tau_{ft}} - 1\right) \quad h > 0, \qquad 0 \text{ otherwise;}$$

$$\rho_s = \frac{2\alpha}{g}(|\boldsymbol{\tau}| - \tau_t),$$

$$T_s = \frac{2\alpha\,|\mathbf{u}|}{g}\frac{\tau_t}{\gamma(|\boldsymbol{\tau}| - \tau_t)}.$$

[35] When the sand flux has been calculated, the height profile is updated according to the formula:

$$\frac{\partial h}{\partial t} = -\frac{1}{\rho_{\mathrm{sand}}}\mathrm{div}\ \mathbf{q} \quad \text{(A5)}$$

[36] In the last step, avalanches are simulated where necessary. If the slope of the sand surface exceeds the static angle of repose, sand is redistributed according to the sand flux:

$$\mathbf{q}_{\mathrm{aval}} = E\frac{\nabla h}{|\nabla h|}\left(\tanh|\nabla h| - \tanh\left(C\tan\vartheta_{\mathrm{dyn}}\right)\right) \quad \text{(A6)}$$

The surface is repeatedly changed according to equation (A5) using this flux, until the maximum slope is below the dynamic angle of repose, ϑ_{dyn}. The hyperbolic tangent functions and the constant $C < 1$ serve only to improve convergence.

[37] All these steps are repeated iteratively to simulate the evolution of the shape.

[38] **Acknowledgments.** E. J. R. Parteli acknowledges support from CAPES, Brasília, Brasil. K.S.E. was supported by the MGS MOC investigation, Jet Propulsion Laboratory contract 959060 to Malin Space Science Systems, Inc.

References

Anderson, R. S., and P. K. Haff (1988), Simulation of aeolian saltation, *Science*, *241*, 820–823.

Anderson, R. S., and P. K. Haff (1991), Wind modification and bed response during saltation of sand in air, *Acta Mech.*, *1*, Suppl., 21–51.

Andreotti, B. (2004), A two-species model of aeolian sand transport, *J. Fluid Mech.*, *510*, 47–70, doi:10.1017/S0022112004009073.

Andreotti, B., and P. Claudin (2002), Selection of dune shapes and velocities. part 2: A two-dimensional modelling, *Eur. Phys. J. B*, *28*, 341–352.

Arvidson, R. E., J. L. Gooding, and H. J. Moore (1989), The Martian surface as imaged, sampled, and analyzed by the Viking landers, *Rev. Geophys.*, *27*(1), 39–60.

Arvidson, R. E., et al. (2004), Localization and physical properties experiments conducted by Spirit at Gusev crater, *Science*, *305*, 821–824.

Bagnold, R. A. (1941), *The Physics of Blown Sand and Desert Dunes*, Methuen, New York.

Bandfield, J. L. (2002), Global mineral distributions on Mars, *J. Geophys. Res.*, *107*(E6), 5042, doi:10.1029/2001JE001510.

Bourke, M., M. Balme, R. A. Beyer, K. K. Williams, and J. Zimbelman (2004), How high is that dune? A comparison of methods used to constrain the morphometry of aeolian bedforms on Mars, in *Lunar Planet Sci.*, *XXXV*, 1713.

Cantor, B. A., P. B. James, M. Caplinger, and M. J. Wolff (2001), Martian dust storms: 1999 Mars Orbiter Camera observations, *J. Geophys. Res.*, *106*(E10), 23,653–23,688.

Cantor, B., M. Malin, and K. S. Edgett (2002), Multiyear Mars Orbiter Camera (MOC) observations of repeated Martian weather phenomena during the northern summer season, *J. Geophys. Res.*, *107*(E3), 5014, doi:10.1029/2001JE001588.

Clark, B. C., A. K. Baird, R. J. Weldon, D. M. Tsusaki, L. Schnabel, and M. P. Candelaria (1982), Chemical composition of Martian fines, *J. Geophys. Res.*, *87*, 10,059–10,067.

Edgett, K. S. (2002), Low-albedo surfaces and eolian sediment: Mars Orbiter Camera views of western Arabia Terra craters and wind streaks, *J. Geophys. Res.*, *107*(E6), 5038, doi:10.1029/2001JE001587.

Edgett, K. S., and P. R. Christensen (1991), The particle size of Martian aeolian dunes, *J. Geophys. Res.*, *96*(E5), 22,765–22,776.

Edgett, K. S., and P. R. Christensen (1994), Mars aeolian sand: Regional variations among dark-hued crater floor features, *J. Geophys. Res.*, *99*(E1), 1997–2018.

Edgett, K. S., and M. C. Malin (2000), New views of Mars eolian activity, materials, and surface properties: Three vignettes from the Mars Global Surveyor Mars Orbiter Camera, *J. Geophys. Res.*, *105*(E1), 1623–1650.

Edgett, K. S., R. M. E. Williams, M. C. Malin, B. A. Cantor, and P. C. Thomas (2003), Mars landscape evolution: Influence of stratigraphy on geomorphology in the north polar region, *Geomorphology*, *52*, 289–297.

Ellwood, J. M., P. D. Evans, and I. G. Wilson (1975), Small scale aeolian bedforms, *J. Sediment. Petrol.*, *45*(2), 554–561.

Finkel, H. J. (1959), The barchans of southern Peru, *J. Geol.*, *67*, 614–647.

Fishbaugh, H. J., and J. W. Head (2005), Origin and characteristics of the Mars north polar basal unit and implications for polar geologic history, *Icarus*, *174*, 444–474.

Fowler, A. C. (2001), Dunes and drumlins, in *Geomorphological Fluid Mechanics*, edited by A. Provenzale and N. Balmforth, pp. 430–454, Springer, New York.

Fryberger, S. G., and G. Dean (1979), Dune forms and wind regime, in *A Study of Global Sand Seas*, edited by E. D. McKee, *U.S. Geol. Surv. Prof. Pap.*, 1052, 137–169.

Greeley, R., M. Kraft, R. Sullivan, G. R. Wilson, N. T. Bridges, K. E. Herkenhoff, R. O. Kuzmin, M. C. Malin, and A. W. Ward (1999), Aeolian features and processes at the Mars Pathfinder landing site, *J. Geophys. Res.*, *104*(E4), 8573–8584.

Hastenrath, S. L. (1967), The barchans of the Arequipa region, southern Peru, *Z. Geomorphol.*, *11*, 300–331.

Hersen, P., K. H. Anderson, H. Elbelrhiti, B. Andreotti, P. Claudin, and S. Douady (2004), Corridors of barchan dunes: Stability and size selection, *Phys. Rev. E*, *69*, 011,304.

Hunt, J. C. R., S. Leibovich, and K. J. Richards (1988), Turbulent shear flows over low hills, *Q. J. R. Meteorol. Soc.*, *114*, 1435–1470.

Iversen, J. D., and B. R. White (1982), Saltation threshold on Earth, Mars and Venus, *Sedimentology*, *29*, 111–119.

Jakosky, B. M., and P. R. Christensen (1986), Global duricrust on Mars: Analysis of remote sensing data, *J. Geophys. Res.*, *91*, 3547–3559.

Kerr, R. C., and J. O. Nigra (1952), Eolian sand control, *Am. Assoc. Pet. Geol. Bull.*, *36*, 1541–1573.

Kroy, K., G. Sauermann, and H. J. Herrmann (2002), Minimal model for aeolian sand dunes, *Phys. Rev. E*, *66*, 031,302.

Lancaster, N. (1989), Star dunes, *Prog. Phys. Geogr.*, *13*, 67–91.

Langevin, Y., F. Poulet, J.-P. Bibring, and B. Gondet (2005), Sulfates in the north polar region of Mars detected by OMEGA/Mars Express, *Science*, *307*, 1584–1586, doi:10.1126/science.1109091.

Long, J. T., and R. P. Sharp (1964), Barchan-dune movement in Imperial Valley, California, *Geol. Soc. Am. Bull.*, *75*, 149–156.

Marchenko, A. G., and A. A. Pronin (1995), Study of relations between small impact craters and dunes on Mars, in *Abstracts of the 22nd Russian-American Microsymposium on Planetology*, pp. 63–64, Vernadsky Inst., Moscow.

Moore, H. J. (1985), The Martian dust storm of Sol 1742, *J. Geophys. Res.*, *90*(S9), 163–174.

Moore, H. J., D. B. Bickler, J. A. Crisp, H. J. Eisen, J. A. Gensler, A. F. C. Haldemann, J. R. Matijevic, L. K. Reid, and F. Pavlics (1999), Soil-like deposits observed by Sojourner, the Pathfinder rover, *J. Geophys. Res.*, *104*(E4), 8729–8746.

Nalpanis, P., J. C. R. Hunt, and C. F. Barrett (1993), Saltating particles over flat beds, *J. Fluid Mech.*, *251*, 661–685.

Owen, P. R. (1964), Saltation of uniform grains in air, *J. Fluid Mech.*, *20*(2), 225–242.

Parteli, E. J. R., V. Schatz, and H. J. Herrmann (2005), Barchan dunes on Mars and on Earth, in *Proceedings of Powders and Grains Conference 2005*, vol. 2, pp. 959–962, Univ. Stuttgart, Stuttgart, Germany.

Sauermann, G. (2001), Modeling of wind blown sand and desert dunes, Ph.D. thesis, Balkema, Leiden, Germany.

Sauermann, G., K. Kroy, and H. J. Herrmann (2001), A continuum saltation model for sand dunes, *Phys. Rev. E*, *64*, 031305.

Schwämmle, V. (2002), Modeling of dune morphology, Diploma thesis, Univ. Stuttgart, Stuttgart, Germany.

Schwämmle, V., and H. J. Herrmann (2003), Solitary wave behaviour of dunes, *Nature*, *426*, 619–620.

Schwämmle, V., and H. J. Herrmann (2004), Modelling transverse dunes, *Earth Surf Processes Landforms*, *29*(6), 769–784.

Schwämmle, V., and H. J. Herrmann (2005), A model of barchan dunes including lateral shear stress, *Eur. Phys. J. E*, *16*, 57–65, doi:10.1140/epje/e2005-00007-0.

Sharp, R. P. (1966), Kelso dunes, Mojave Desert, California, *Geol. Soc. Am. Bull.*, *77*, 1045–1074.

Sullivan, R., R. Greeley, M. Kraft, G. Wilson, M. Golombek, K. Herkenhoff, J. Murphy, and P. Smith (2000), Results of the Imager for Mars Pathfinder windsock experiment, *J. Geophys. Res.*, *105*(E10), 24,547–24,562.

Thomas, M., J. D. A. Clarke, and C. F. Pain (2005), Weathering, erosion and landscape processes on Mars identified from recent rover imagery, and possible Earth analogues, *Aust. J. Earth Sci.*, *52*, 365–378, doi:10.1080/08120090500134597.

Tsoar, H. (1982), Internal structure and surface geometry of longitudinal seif dunes, *J. Sediment. Petrol.*, *52*, 823–831.

Tsoar, H. (1983), Dynamic processes acting on a longitudinal (seif) sand dune, *Sedimentology*, *30*, 567–578.

Tsoar, H. (1989), Linear dunes—Forms and formation, *Prog. Phys. Geogr.*, *13*, 507–528.

Tsoar, H., R. Greeley, and A. R. Peterfreund (1979), Mars: The north polar sand sea and related wind patterns, *J. Geophys. Res.*, *84*(B14), 8167–8180.

Weng, W. S., J. C. R. Hunt, D. J. Carruthers, A. Warren, and G. F. S. Wiggs (1991), Air flow and sand transport over sand-dunes, *Acta Mech.*, Suppl. 2, 1–22.

Zimbelman, J. R. (2000), Non-active dunes in the Acheron Fossae region of Mars between the Viking and Mars Global Surveyor eras, *Geophys. Res. Lett.*, *27*(7), 1069–1072.

K. S. Edgett, Malin Space Science Systems, P.O. Box 910148, San Diego, CA 92191-0148, USA.

H. J. Herrmann, E. J. R. Parteli, and V. Schatz, Institute for Computational Physics, Stuttgart University, Pfaffenwaldring 27, D-70569 Stuttgart, Germany. (schatz@ica1.uni-stuttgart.de)

H. Tsoar, Department of Geography and Environmental Development, Ben Gurion University of the Negev, Beer Sheva, 84105 Israel.